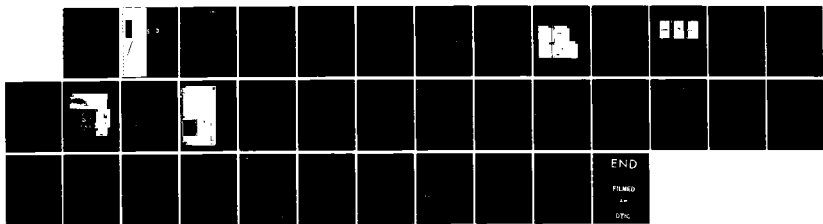
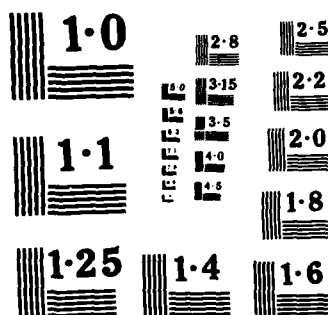


RD-A162 858 MEGA-AMP OPENING SWITCH WITH NESTED ELECTRODES/PULSED 1/1
GENERATOR OF ION AN. (U) STEVENS INST OF TECH HOBOKEN N
J V NARDI ET AL. 01 JUL 85 AFOSR-TR-85-1125
UNCLASSIFIED AFOSR-84-0228 F/G 20/9 NL

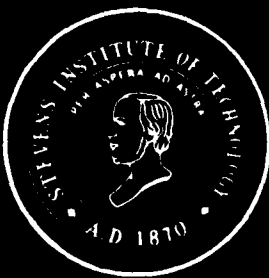


END
FILED
--
DPC



NATIONAL BUREAU OF STANDARDS
MICROCOPY RESOLUTION TEST CHART

AD-A162 850



STEVENS INSTITUTE
OF TECHNOLOGY

CASTLE POINT STATION
NEWARK, NEW JERSEY 07030

AFOSR-TR- 85-1125

SIT-AFOSR-N-84.85.4

Mega-Amp Opening Switch with
Nested Electrodes/Pulsed Generator
of Ion and Ion Cluster Beams

DTIC
ELECTED
DEC 31 1985
S D
D

• V. Nardi

July 1, 1985

Annual Report
for the period
July 1, 1984 - June 30, 1985

AFOSR 1984-1985

Grant No. AFOSR-84-0228

85 12 30 017

UNCLASSIFIED

AD-1162850

2

SECURITY CLASSIFICATION OF THIS PAGE

REPORT DOCUMENTATION PAGE

1a. REPORT SECURITY CLASSIFICATION Unclassified		1b. RESTRICTIVE MARKINGS	
2a. SECURITY CLASSIFICATION AUTHORITY		3. DISTRIBUTION/AVAILABILITY OF REPORT Approved for public release; distribution unlimited.	
2b. DECLASSIFICATION/DOWNGRADING SCHEDULE			
4. PERFORMING ORGANIZATION REPORT NUMBER(S)		5. MONITORING ORGANIZATION REPORT NUMBER(S) AFOSR/NP 85-1125	
6a. NAME OF PERFORMING ORGANIZATION Stevens Institute of Technology	6b. OFFICE SYMBOL (If applicable)	7a. NAME OF MONITORING ORGANIZATION AFOSR/NP	
6c. ADDRESS (City, State and ZIP Code) Stevens Institute of Technology Castle Point, Hoboken, NJ 07030		7b. ADDRESS (City, State and ZIP Code) Building 410 Bolling AFB, DC 20332-6448	
8a. NAME OF FUNDING/SPONSORING ORGANIZATION AFOSR	8b. OFFICE SYMBOL (If applicable) NP	9. PROCUREMENT INSTRUMENT IDENTIFICATION NUMBER AFOSR-84-0228	
8c. ADDRESS (City, State and ZIP Code) Building 410 Bolling AFB, DC 20332-6448		10. SOURCE OF FUNDING NOS. PROGRAM ELEMENT NO. 61102F PROJECT NO. 2301 TASK NO. A7 WORK UNIT NO. N/A	
11. TITLE (Include Security Classification) "MEGA-AMP OPENING SWITCH WITH NESTED ELECTRODES/PULSED GENERATOR OF ION AND ION CLUSTER BEAMS"			
12. PERSONAL AUTHOR(S) C.M. Lou, V. Nardi, C. Powell			
13a. TYPE OF REPORT Annual	13b. TIME COVERED FROM 01-07-84 TO 30-06-85	14. DATE OF REPORT (Yr., Mo., Day) 85-07-01	15. PAGE COUNT 33
16. SUPPLEMENTARY NOTATION			
17. COSATI CODES		18. SUBJECT TERMS (Continue on reverse if necessary and identify by block number)	
FIELD	GROUP	SUB. GR.	
19. ABSTRACT (Continue on reverse if necessary and identify by block number) During the first year of the research program on the use of a plasma focus machine (PF) as a M Amp opening switch we have: (A) Improved the performance of our presently functioning system by finding a new method of increasing the surge of anomalous (i.e., noncollisional) resistivity which controls the "switch opening" function (specifically, the rate of disintergration of the PF pinch where the current is concentrated). (B) Devised new methods to monitor the rate of disintegration of the PF pinch via the changes of the particle emission spectra as a function of time (on a nanosec scale) and of position (on a 50 micrometer scale) inside the pinch. (C) Made substantial progress in the construction of an upgraded system which can operate at higher current levels as compared to the present 0.5 - 0.7 MA.			
20. DISTRIBUTION/AVAILABILITY OF ABSTRACT UNCLASSIFIED/UNLIMITED <input checked="" type="checkbox"/> SAME AS RPT. <input checked="" type="checkbox"/> DTIC USERS <input type="checkbox"/>		21. ABSTRACT SECURITY CLASSIFICATION UNCLASSIFIED	
22a. NAME OF RESPONSIBLE INDIVIDUAL MAJ, BRUCE L. SMITH		22b. TELEPHONE NUMBER (Include Area Code) 202-767-4906	22c. OFFICE SYMBOL NP

Mega-Amp Opening Switch with Nested Electrodes/Pulsed

Generator of Ion and Ion Cluster Beams

V. Nardi

Report for the Period July 1, 1984-June 30, 1985

Information and experimental data entered in this report

have been contributed by

C. M. Luo, V. Nardi, C. Powell

AFOSR 1984-1985

Grant No. AFOSR-84-0228

AIR FORCE OFFICE OF SCIENTIFIC RESEARCH AFOSR
REPORT

Accesion For	
NTIS	CRA&I
DTIC	TAB
Unannounced	
Justification	
By	
Distribution	
Availability Codes	
Dist	Available or Special
A-1	

July 1, 1985



p. 1-33

Mega-Amp Opening Switch with Nested Electrodes/Pulsed Generator of Ion and Ion Cluster Beams

Section 1. Summary

During the first year of the research program on the use of a plasma focus machine (PF) as a M Amp opening switch we have:

- (A) Improved the performance of our presently functioning system by finding a new method of increasing the surge of anomalous (i.e., noncollisional) resistivity which controls the "switch opening" function (specifically, the rate of disintegration of the PF pinch where the current is concentrated).
- (B) Devised new methods to monitor the rate of disintegration of the PF pinch via the changes of the particle emission spectra as a function of time (on a nanosec scale) and of position (on a 50 micrometer¹ scale) inside the pinch.
- (C) Made substantial progress in the construction of an upgraded system which can operate at higher current levels (about $\gtrsim 2$ MA) as compared to the present 0.5 - 0.7 MA.

(A) has been accomplished by introducing a field distortion element at the breech of the coaxial electrode system. Specifically, a circular knife edge of conducting material has been inserted on the insulator sleeve between the electrodes where the field distribution is the main controlling factor of the structure (thickness) of the plasma current sheath between the electrodes. The smaller is the thickness of the PF current sheath at all stages of the interelectrode current pulse (for a fixed value of the interelectrode peak current) the higher is the surge of anomalous resistivity at the peak of the current pulse.

(B) is based on the determination of ion emission spectra from the PF pinch from compact Thomson spectrometers with a nanosec time resolution and from a high resolution magnetic analyzer with focalization of the ion beams in the field edge of the pole pieces. Time resolution on the Thomson spectrometer is obtained by a ramped field applied to the spectrometer pole pieces.

(C) consists of the construction of five (MA) closing switches to power the upgraded 50 - 200 kJ PF system and of the trigger system of the five switches

(with gitter \approx 5-10 μ s). This is necessary for tests on scaling of switch performance with current-pulse amplitude and for tests on the nested electrode geometry, with more than two coaxial electrodes.

The variation with time (t) of the current I on the PF electrodes (and of the corresponding magnetic field B) is monitored via the time-derivative signal ($dI/dt \sim dB/dt$) from a 70 cm long Rogowski belt (+) located near the PF closing switch between the capacitor bank and the PF electrodes [$I(t)$ is also determined via a Rogowski belt encircling one of the two plates which feed the PF electrodes]. Empirical relationships between the rate of decrease of I (and the net decrease of I) as a consequence of the PF pinch breakdown* and the D-D neutron yield n (with a D_2 filling of the PF discharge chamber, n = neutron count - in one discharge of the capacitor bank - from a Los Alamos silver-activation counter) have been established in previous work from the polynomial representation $|dI/dt| \sim A[t(ns)+150]^\gamma$. In this expression $t=0$ coincides with the time at which the absolute value $|dI/dt|$ has the first sharp peak; t is measured in nanosec, γ is determined from a best fit of the observed signal in the time interval from $t = -150$ ns to $t=0$. By plotting the values of n from many shots as a function of γ it was found that n is a monotonically increasing function of γ (and γ is an increasing function of n ; typically $3 \leq \gamma \leq 5$ for the discharge conditions reported here). Consistently with this result we find convenient (with a fixed set of values the capacitor bank energy and of other typical PF parameters) to use n as a suitable quantity for a quantitative description of the circuit-opening function of the PF. In Section 2 we report the data from PF discharges with the circular knife edge on the insulator sleeve. Data on the characteristic of the ion emission from the PF pinch are reported in Section 3 and 4. Sections 2 and 3 address the specific topics i.e., to the influence of the knife edge distortion field on the pinch structure during pinch breakdown and to ion source structure/ion energy spectrum anisotropy respectively. Section 4 provides technical details on the method for obtaining data reported in Sections 2,3 with a review of the general approach. The method to achieve time resolution in the ion-spectrum determination is also reported in Section 4. Figure, captions and bibliography are listed separately for each Section.

(+) with 60 turns, single loop dia. 1.4 mm.

* On which the "circuit-opening function" of the PF is based.

1. V. Nardi, W. H. Bostick, J. Feugeas, W. Prior, C. Cortese, Nuclear Fusion, Suppl. Vol. 2, p. 143 (1979).

Section 2.

Pinhole camera photographs are taken at 0° , 45° , 80° from the x-ray emission and ion emission of a single PF discharge by using a sandwich of x-ray film and CR-39. Energy analysis is obtained with a magnet behind the pinhole and filters. A metallic circular knife edge is used on the insulator sleeve for increasing the neutron yield. A specific effect of knife edge on the ion image is observed.

1. The pinhole camera and the x-ray and CR-39 sandwich arrangement is the same as described in Ref. 1. A circular knife edge (KE) of conducting material is fitted on the insulator sleeve (as indicated in Fig. 1). The KE increases the neutron yield as reported from the data in Fig. 2. Different values L of the KE length have been tested with an overall better performance for $L = 7-8$ mm at a capacitor bank voltage of $V = 17$ KV (8-10 kJ, $V = 15-17$ KV) and a filling of D_2 at a pressure $P \geq 6$ Torr. This conclusion has been reached by a series of tests (4000 shots of two identical Mather type machines at Stevens Tech - STI and at the University of Ferrara* - UF) for different values of VLP.

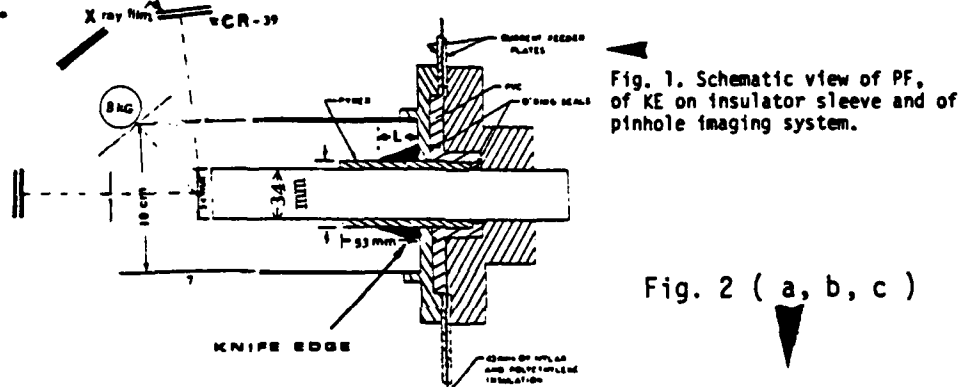
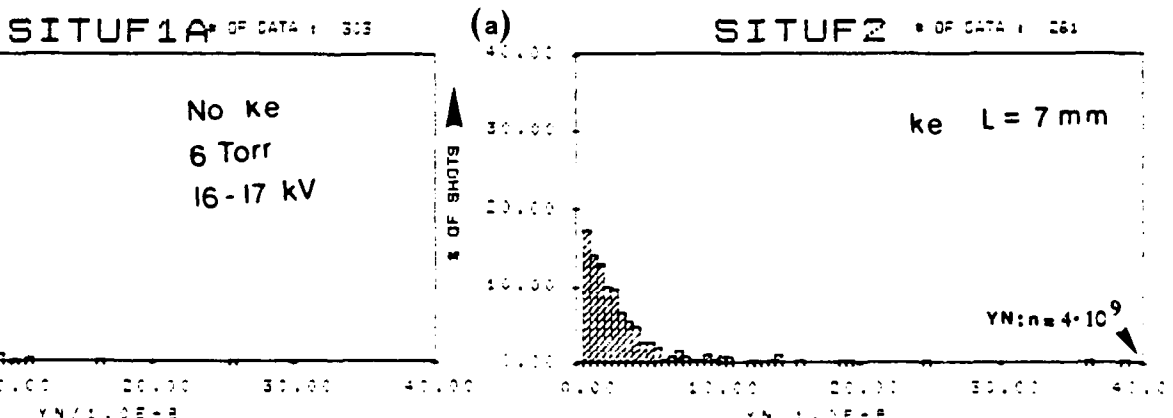


Fig. 1. Schematic view of PF, of KE on insulator sleeve and of pinhole imaging system.

Fig. 2 (a, b, c)



* In order to reduce the importance of statistical fluctuations in the preparation of the diagrams of Fig. 2 we have entered in Fig. 2-also data from PF discharges of a PF machine of the University of Ferrara (UF) with identical geometry, capacitor bank and operating conditions of the PF at Stevens Tech (SIT).

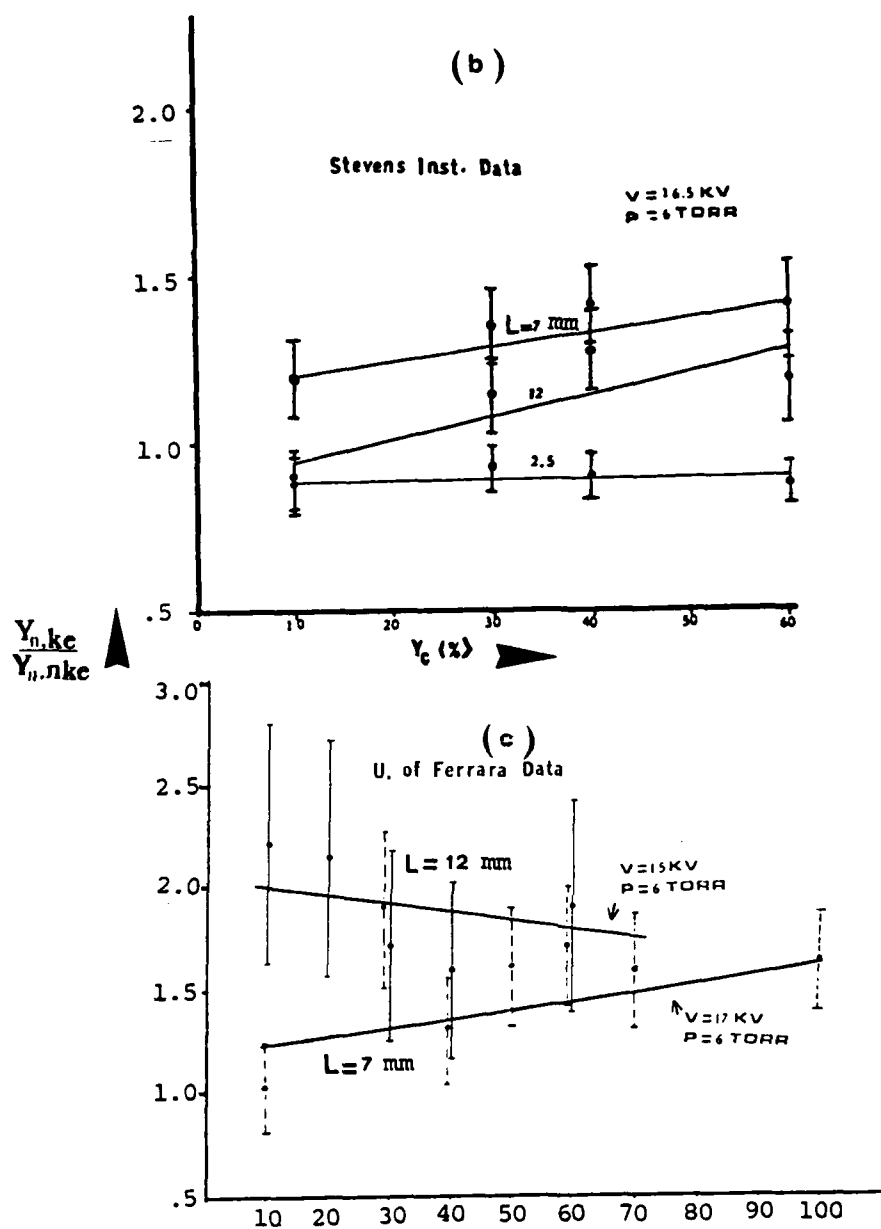
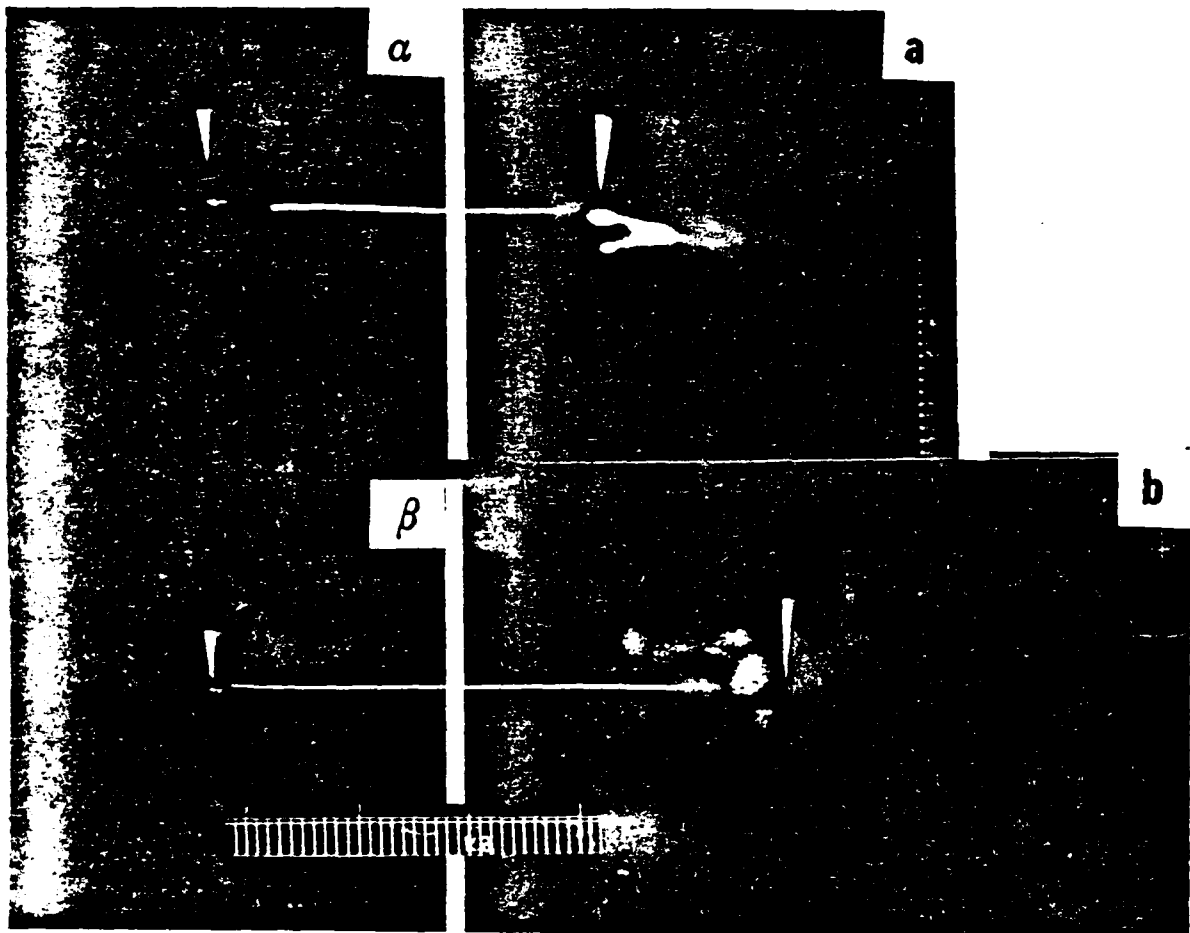


Fig. 2(a) Histogram of data from SIT and Univ. of Ferrara data without (1A) and with KE (2); (b) and (c) report data for different set of VPL separately from SIT and UF, specifically:

Ratio of the neutron yield from shots in which a knife edge is used [$Y_{n,ke}(y_c)$] and from shots without knife edge [$Y_{n,nke}(y_c)$] as a function of a chosen yield y_c . $Y_n(y_c)$ is the mean value of the neutron yield for all and only the shots with a neutron yield above or at least equal to a chosen yield y_c ; y_c is expressed as a percentage of the "peak yield" $y_{n,max}$. As a definition of $y_{n,max}$ for a specific set of values V, P, L we take here the mean value of the yield from the three shots with the highest neutron yield for the same set of values of V, P, L .

Fig. 3. (α), (β): pinhole camera image from the x-ray emission (α) at 80°, (β) at 45° (pinhole dia. $\sim 300 \mu\text{m}$ at 80°, $150 \mu\text{m}$ at 45°); the thickness of the filter for the x-ray image is equivalent to 1.5-2 mm Be ($\sim 10 \text{ keV}$ x-rays); in (a) 80° and (b) 45°, same view but from ion track image on CR-39. The horizontal axis marks the axis of the discharge. The vertical arrows mark the axial coordinate of corresponding points in (α,a) and (β,b) respectively. No knife edge used in this shot.



These type of tests have been carried out with two objectives in mind: (a) to have a quantitative assessment of the effect on the neutron yield (i.e., on PF optimization) of the knife edge (KE) which is now used in different laboratories. (b) To observe typical variations of the PF pinch configuration (from pinhole camera images) which can be induced by using a KE (with "PF optimization" - for a given capacitor bank and peak voltage V - we mean here the conditions on D_2 filling pressure, electrode and insulator parameters, inductance value which lead to a maximum of electrode and of pinch current at a suitable time for having a maximum neutron yield). A substantial increase of the neutron yield (typically by a factor 1.6-2.5) is observed in the mean value of the yield from a series of many (~ 250-300) shots for a fixed set of V, P (15-17kV, 5-6Torr) if a KE ($L=7-12$ mm) is used as compared to the configuration without KE. The increase is even higher (by a factor ~ 2.5-4) if maximum values of the yield are compared for the two configurations. As a standard procedure in each series we have alternate runs of about 20 shots without KE with runs of ~20 shots with KE, and with D_2 refilling after each run. This eliminates biasing effects, e.g., of the spark plug erosion in open-air switch, of the PF electrode and insulator "aging" under discharge conditions, and of impurity contamination of the discharge-chamber fillings (these effects are partially responsible for the fluctuations of the neutron yield observed for each set V, P, L). The pressure was monitored after each shot. An increase of pressure up to ~5% of the filling pressure was observed after some of the peak-yield shots. In the tests reported here D_2 refilling was carried out also any time the wall outgassing increased the discharge-chamber pressure above 3% of the filling pressure. Results from the method of obtaining the image of the PF pinch simultaneously from x-ray emission and from particle emission with a sandwich of one x-ray film (back) and CR-39 target (front) has been reported in Ref.1. Three sandwiches have been routinely used ($0^\circ, 45^\circ, 80^\circ$) and a 8kG magnetic field orthogonal to the line of sight is inserted immediately behind the pinhole. Typical results are reported in Figures 3,4. We note that the ion image at 80° is usually sifted of about 1-2mm below the corresponding x-ray image which is on the discharge (electrode) axis. In the image at 45° the x-ray point source has an axial coordinate near the middle of one of the two ion images in which the original image (i.e. the image we would obtain without the 8kG magnet) is splitted from the 8kG magnetic field. The particle image with the same coordinates of the x-ray image is referred to as the unshifted image (UI). The UI is formed of large diameter ion tracks (dia. $8-12\mu\text{m}$). The shifted image (SI) is formed from D^+ ion tracks with dia. $2-6\mu\text{m}$ under our CR-39 etching conditions (3 hours in a 700°C NaOH solution, 6.25 normal). UI is formed of tracks of ions with $m/z \gg 1$ and is wiped out from a formvar filter $0.1\mu\text{m}$ thick, whereas the SI is wiped out (at least partially) from a mylar filter of thickness $\sim 50\mu\text{m}$ (range of D^+ ions with energy ~2.4 MeV). The energy of the particles is changing with the axial coordinate in both SI and UI. The maximum particle energy is on the sharp part of the image, on the image side away from the center electrode. This is confirmed by filter data 1. The image in Fig. 3 is obtained without KE. In shots without KE the axially elongated UI and the SI are generally parallel to each other along the electrode axis. A systematic variation is introduced from the KE. Specifically the 45° SI is tapered away from the anode; SI is at an angle (~ 30°) with respect to the electrode axis (and to UI) and merges with UI on the axis, at the image side of peak particle energy, away from the

anode. This change from parallel configuration (without KE) to oblique configuration with a KE is observed in 90% of the obtained images (about 100 images sofar). Our data confirm that the KE changes the current sheath structure in a definite manner and that these structural changes are usually associated with an increase of the neutron yield.

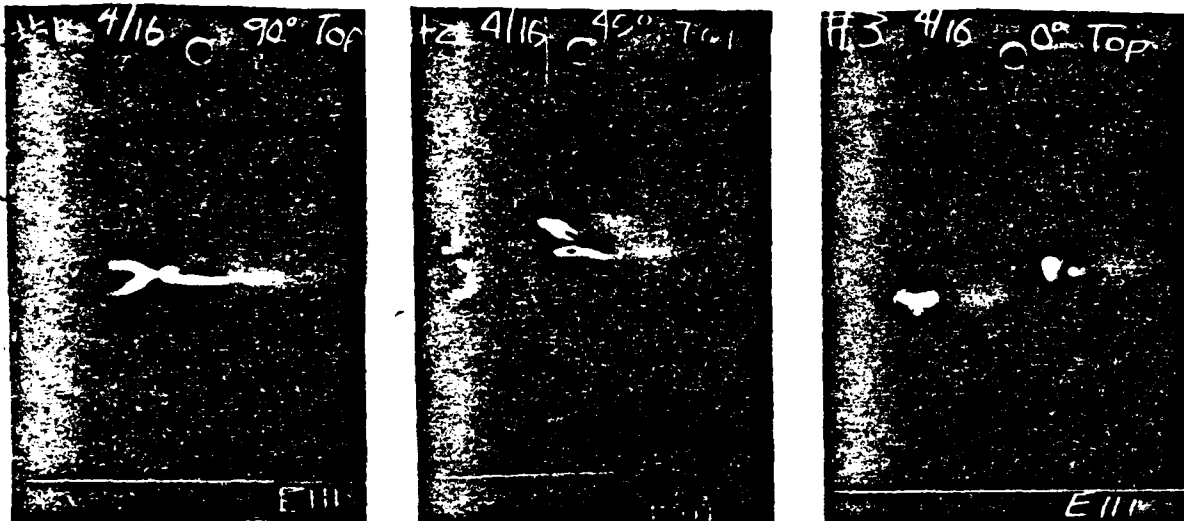


Fig. 4. Pinhole image of the PF pinch from ion tracks on CR-39 (80° , 45° , 0°) respectively. Knife edge was used in this shot (note typical inclination of shifted image) with respect to axis. Maximum particle energy on right side tip. Scalloped areas of track saturation visible in shifted image.

References

1. W. H. Bostick, et al. Energy Storage, Compression and Switching, Vol. 2, Plenum, N.Y., 1983. V. Nardi, C. Powell, W. Prior and W. H. Bostick, Proc. Europ. Conf. on Fusion, Aachen, Vol. 7D, part 1, pg. 489 (1983).
2. S. Denus: Review of Plasma Focus Research at the IPPLM; Proc. 3rd Int. Workshop on Plasma Focus Research (Univ. of Stuttgart) Sept. 1983, IPF - 83-6 Report.

Section 3.

The intensity and the energy spectrum $N_\alpha(E)dE$ (60 keV $\lesssim E \lesssim 1$ MeV) of the D^+ ion emission from plasma focus discharges and of other charged particles has been determined in different directions ($0^\circ, 70^\circ, 180^\circ$) with respect to the electrode/discharge axis. Pinhole images of the pinch from etched ion tracks on CR-39 targets with differential filters provide the structure of the ion source.

1. A compact Thomson spectrometer with an energy resolution $\Delta E/E \approx 1-6\%$ is used to determine the energy spectrum of D^+ ions (and of other charged particles with a mass/charge ratio $m/z \geq 1$) ejected from a plasma focus (PF) pinch (8-10 kJ at 15 kV-17 kV; see Fig. 1) at $0^\circ, 70^\circ, 180^\circ$ with respect to the electrode axis. A collimated electron beam (REB) composed of multiple $\approx 1-10$ ns pulses is also emitted in the 180° direction from a plasma source localized in the same region of space of the ion source. The REB has a broad energy spectrum peaked between 0.3 MeV-0.7 MeV. Collective field acceleration of ions from the background gas in the drift chamber (same filling gas and pressure P of the PF pinch chamber) is observed at 180° along the REB propagation path.^{1,2} A method is outlined here for discriminating collectively accelerated ions at 180° which form the bulk of the ion population at $E \gtrsim 1$ MeV and ions emitted from the PF source. Fig. 2 reports a pinhole image of the pinch ($80^\circ, 45^\circ, 0^\circ$ views) from ion emission. The pinholes (dia. 150 μm at $0^\circ, 45^\circ$; 200 μm at 80°) are at the same distance (7.5 cm) from source and CR-39 targets. Two circular pole pieces (dia. 2.5 cm) with a 8 kG uniform field in the pole cylindrical gap is located immediately behind the 45° pinhole. This field splits the image in two images both with sharp boundaries. The undeflected image is formed by non uniform distribution of ion tracks of large diameter ($\approx 9-12 \mu m$); the deflected image is formed by D^+ ion tracks (2-5 μm dia) - if deuterium filling is used - from ions with different energy values (100 keV $\lesssim E \lesssim 3.5$ MeV). A grid of cylindrical yarns (yarn dia. 50 μm) screens out ions of relatively low energy and provides the dimensions of the region where high energy ions are emitted. This filter does not wipe out the image of the pinch as a continuous filter would do. In Fig. 3 we report Thomson spectrometer data at 0° . Two configurations (A), (B) of the Thomson spectrometer have been used: In (A) the spectrometer pinhole (ph-I) is located before the spectrometer magnetic pole pieces (the electric field V_T of the spectrometer is also applied between these pole pieces); in (B) ph-I is located near the CR-39 target (T) downstream of the pole pieces (Rhee configuration)³. In order to have reliable results with configuration (B) it is necessary to have a uniform ion "illumination" of the entrance aperture of the spectrometer, i.e., on a surface \approx cross section of spectrometer interelectrode gap (cross section orthogonal to the beam direction). This condition is not satisfied in our experiments and, we believe, in all experiments with plasma focus systems even if a number of shots larger than 10 or 20 is used to obtain the

spectrum. This can be shown for example by comparing typical spectra from (A) with typical spectra from (B) in discharge with a filling mixture, e.g., of 30% of H_2 and 70% of D_2 by pressure P . We observe that B gives a parabola for H^+ within ion track density higher than for D^+ ions for all observed values of the ion energy E whereas the ion track density on the H^+ and D^+ parabolas from (A) fits closely the fractional composition of the source (scattering of H^+ ions before the entrance of the Thomson spectrometer is partially responsible for the discrepancy between (A) and (B) data). Fig. 3-b reports the ion spectrum at 70° and Fig. 3-c that at 180° . Collective field acceleration from the REB field at 180° is assessed from different features of the ion spectrum, specifically a higher density of ion tracks is observed in the $\gtrsim 1$ MeV region if a focalization system for the electron beam is used in the REB drift chamber. We explain this systematic variation of the spectrum in terms of collective field acceleration also because the increase in the \gtrsim MeV ion population depends only on the focalization constraints on the REB (e.g., diameter, type of material and termination of the REB drift chamber) which reduce the admittance angle of the Thomson spectrometer without affecting the PF ion and electron beam source.

2. A review of our data, in particular the extremely small cone of emission and the localization of the source regions from which ions with $E \gtrsim 2.4$ MeV are emitted, indicate that the fine structure of the source^{1,4} may affect the spectrum determination by modulating the ion fluence $d^2N/dEd\omega$ on the target on a E, ω scale also smaller than the resolution of the spectrometer. This is the case, e.g., if the emission cone is much smaller than the acceptance angle of the spectrometer and the source "hot spot" has a transverse dimension smaller than the diameter of both pinholes of the spectrometer collimator system as we have frequently observed. Imaging of the source through the spectrometer collimator has been verified in our high resolution magnetic analyzer with edge focusing and ion trajectories ~ 100 cm long in the 10^{-5} vacuum chamber of the analyzer². In that case the width of the elliptically-shaped projection of the collimator aperture on the surface of the target was $\Delta x(x) \gtrsim 1$ cm [the analyzer resolution $\Delta E(\Delta x)/E \gtrsim 0.5-5\%$ is determined by $\Delta x, E$] whereas we have observed regularly-spaced modulations on a 1 mm scale of the etched ion track density for $E \gtrsim 0.5$ MeV.

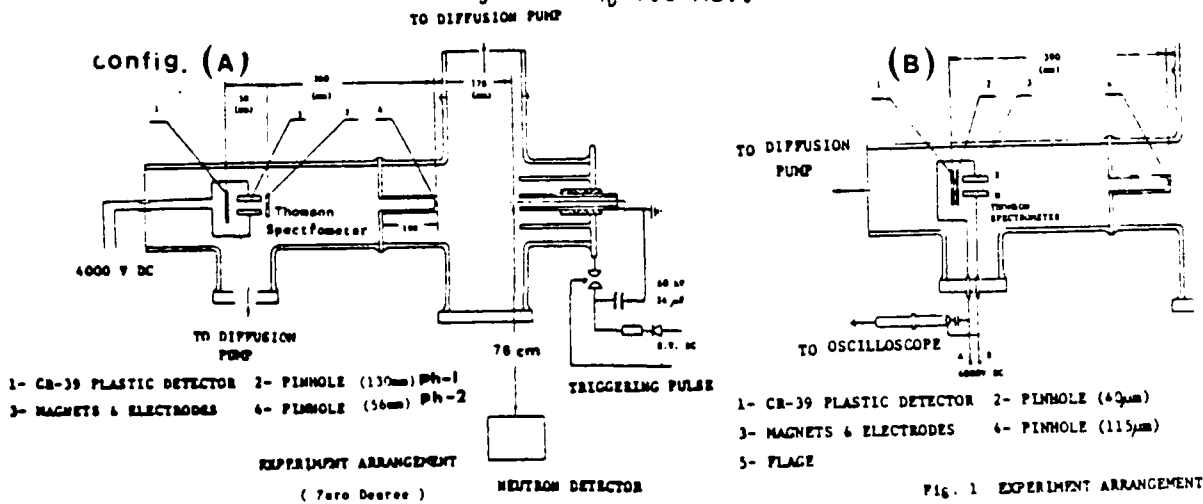
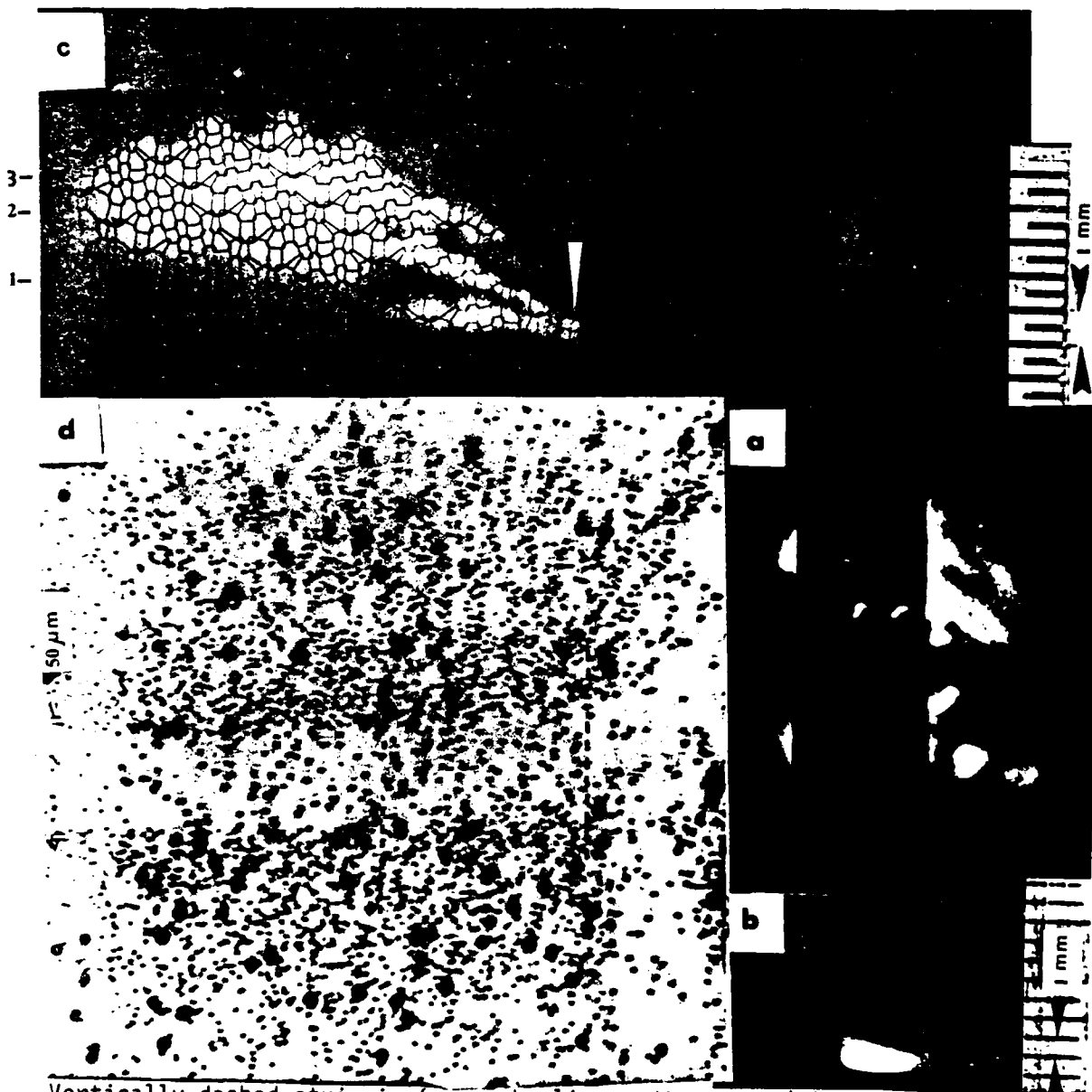


FIG. 1 EXPERIMENT ARRANGEMENT

Fig. 2. Time - integrated pinhole image of the pinch on CR-39 targets: 0° in (a), 80° , 45° (in c) view (same shot). The central filter strip at 0° is $6 \mu\text{m}$ thick ($\approx D^+$ range for $E \sim 0.6 \text{ MeV}$). The white arrow in (c) indicates the location of the microscope photograph in (d). Note outline of grid wire ($\sim 50 \mu\text{m}$ dia.) in (c) which is crossed by D^+ with $E \sim 2.4 \text{ MeV}$. (d) is taken at the point where the image (2)-shifted by the 8kG magnet behind the pinhole-merges with the unshifted image (1) which fits the 10 keV image an axis). The point where (1) and (2) merge is usually a "hot spot" with $E > 2.4 \text{ MeV}$ for D^+ ; other hot spots are detected sometime also near the cusped profile (upper border) of the pinch. The image (3) is formed by ion tracks similar to those in (2); large tracks with dia. $\sim 10 \mu\text{m}$ form (1). Note that the linear dimensions of the $> 2.4 \text{ MeV}$ hot spot in (d) are $\sim 100 \mu\text{m}$, i.e. less than the pinhole diameter $150 \mu\text{m}$ (the pinhole diameter is $\sim 200 \mu\text{m}$ in (a)). The ion acceleration mechanism is localized within regions of space of linear dimensions $\sim 300 \mu\text{m}$ which are embedded in a source of greater linear dimensions ($\sim 1 \text{ cm}$) emitting lower energy ions. This feature (localized "hard" source within a diffuse "soft" source) is also observed in the x-ray bremsstrahlung emission (1-10 keV).



Vertically dashed strip in (a) marks linear dimension (λ) of "hot spot" with peak density of $E \gtrsim 2.4$ MeV D^+ tracks ($\lambda \lesssim 100 \mu\text{m} < \text{pinhole dia. } 150 \mu\text{m}$). Where two wires overlap (middle right of (d)) the filter is $100 \mu\text{m}$ thick (observed tracks fit D^+ with $E \gtrsim 3.6$ MeV); center electrode at left in (b,c,d).

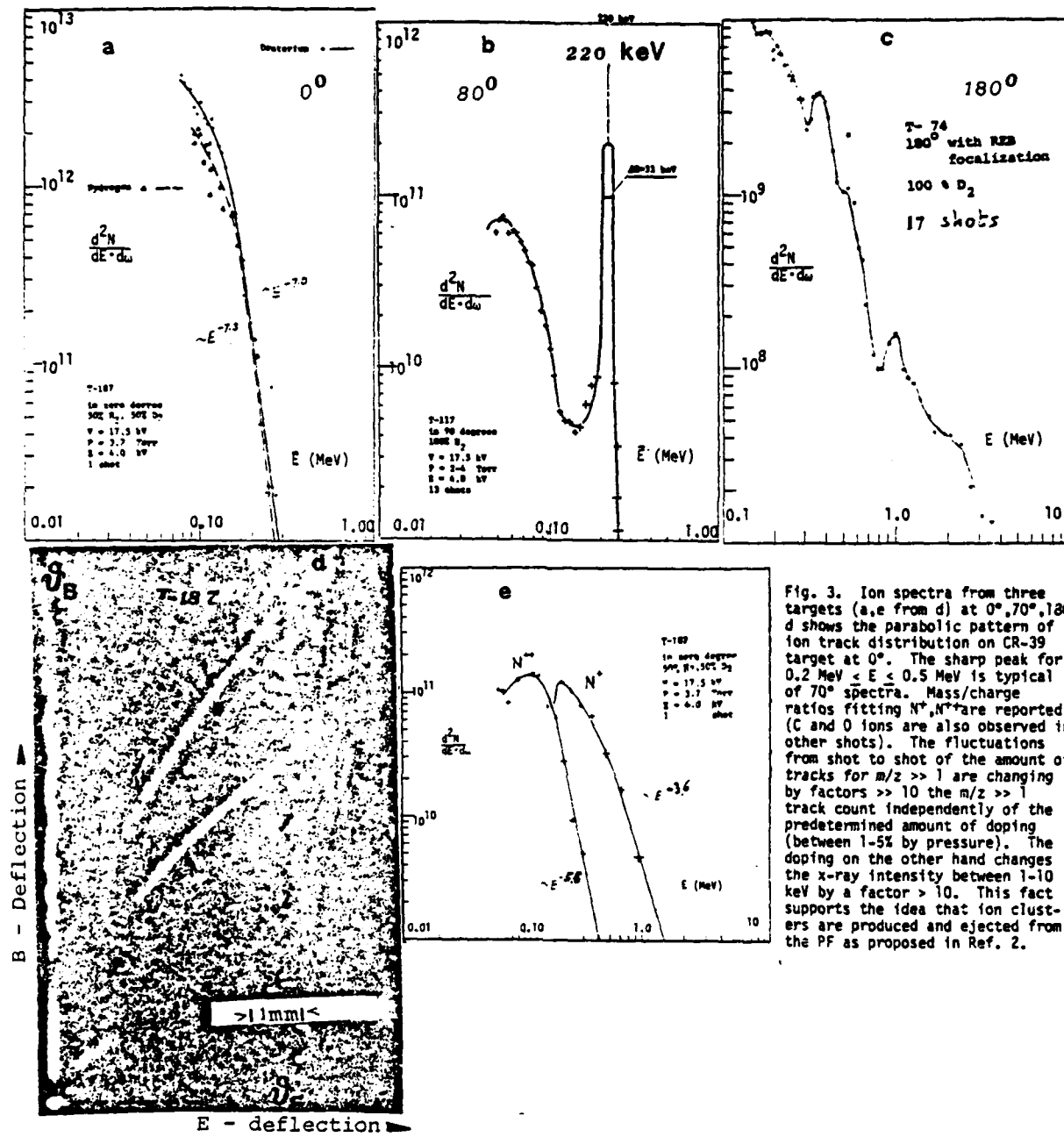
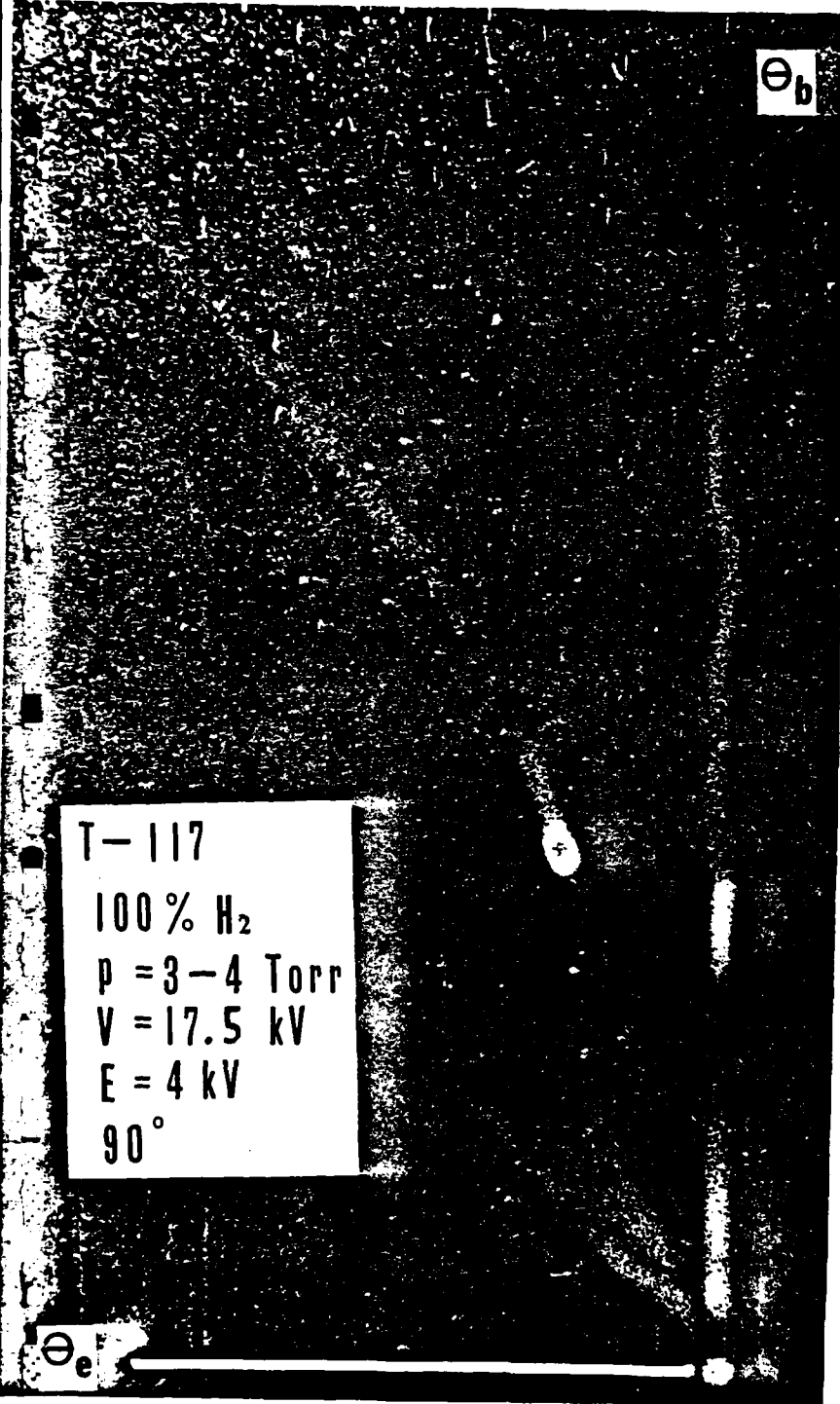


Fig. 3. Ion spectra from three targets (a,e from d) at $0^\circ, 70^\circ, 180^\circ$; d shows the parabolic pattern of the ion track distribution on CR-39 target at 0° . The sharp peak for $0.2 \text{ MeV} < E < 0.5 \text{ MeV}$ is typical of 70° spectra. Mass/charge ratios fitting N^{++}, N^+ are reported. (C and O ions are also observed in other shots). The fluctuations from shot to shot of the amount of tracks for $m/z \gg 1$ are changing by factors $\gg 10$ the $m/z \gg 1$ track count independently of the predetermined amount of doping (between 1-5% by pressure). The doping on the other hand changes the x-ray intensity between 1-10 keV by a factor > 10 . This fact supports the idea that ion clusters are produced and ejected from the PF as proposed in Ref. 2.

References

1. V. Nardi, W. H. Bostick, J. Feugeas, W. Prior, Phys. Rev. 22A, 2211 (1980) and Energy Storage, Compr., Switching, 2, p. 437 (1983), Plenum, N.Y.
2. V. Nardi, C. Powell: A.I.P. Proc. 111, 463 (1984) N.Y., and Proc. Europ. Phys. Soc. Proc. Vol. 7D, part I, p. 489 (1983).
3. R. S. Schneider, C. M. Luo, M. J. Rhee: J. Appl. Phys. 57, 1 (1985). M. J. Rhee: Rev. Sci. Instrum. 55, 1229 (1984).
4. M. Sadowski, H. Herold, H. Schmidt: Phys. Lett. 105A, 117 (1984). S. Czekay, S. Denus et al.: Europhys. Conf. 7D Part 1, 469 (1983).

Fig. 4. Image of target 117 from which we have obtained the spectrum in Fig. 3 (b) .



Section 4.

Interelectrode-field distortion elements (metallic knife edge, A, and necking insert, B, Fig. 1) have been tested in one of the switch basic components, a PF electrode pair with a peak current ≥ 0.5 MA. The purpose was to reduce the thickness of the current sheath (CS) by affecting the CS formation stage during breakdown between electrodes. A thinner CS with a greater current density increases the rate of switching also by increasing the rate of decay of CS in the late stage of axial pinch. All tests have been carried out between 13.5 kV and 17.5 kV with 6 Torr of deuterium filling of the discharge chamber to monitor the opening rate of the current channel from the neutron yield of D-D fusion reactions in parallel with the bremsstrahlung x-ray signal.

The results presented in table I and Fig. 2 indicate an increase of the switching rate [$\sim \int_{t_1}^{t_2} |dI/dt| dt / (t_2 - t_1)$]^{*}, as it is assessed from the increase of the D-D neutron yield] better than 10% from a statistic analysis of eleven hundred shots - and up to 100% for peak yield shots - depending on the length L of the knife edge.

- Anisotropy of the energy spectrum of the ion emission.

We have determined the energy spectrum $N_\alpha(E)dE$ of the ion beams emitted in different directions (α) with respect to the electrode axis ($\alpha = 0^\circ, 90^\circ, 180^\circ$) of a plasma focus discharge (PF) (~ 5 kJ at 20 kV), filling pressure 4 Torr of D_2 or of convenient H_2+D_2 mixtures. We have used Thomson spectrometers for ion-energies $E \geq 70$ keV-1 MeV (all α) and a high resolution magnetic analyzer with field-edge focussing and ion filtering for $E \geq 0.3-8$ MeV ($\alpha = 0^\circ$). The typical spectral amplitude $N_{180}dE$ of the ion beam at 180° (i.e., in the direction in which the PF pinch ejects a collimated ~ 10 kA beam of ~ 400 keV electrons) is smaller than N_0dE with typical values $N_0(0.3 \text{ MeV})/N_{180}(0.3 \text{ MeV}) \approx 100$ but has a relatively-stronger component of high energy ions $N_{180}(0.8 \text{ MeV})/N_{180}(0.1 \text{ MeV}) > 10 N_0(0.8 \text{ MeV})/N_0(0.1 \text{ MeV})$. The source brightness was measured for different α . The angular spread of the 180° ion beam decreases for increasing energy values and is $\ll 1^\circ$ for $E \sim 0.5$ MeV. The spectral resolution $\delta E/E$ of the magnetic analyzer is better than 1% for $1 \text{ MeV} \leq E \leq 7 \text{ MeV}$ and that of the Thomson spectrometer $\sim 10\%$ for $E \sim 0.1 - 0.8$ MeV.

* $|dI/dt|$ is the absolute value of the time derivative of the electrode current I. The time integration is carried out on the time interval t_2-t_1 in which the current is decreased (switched off) to a predetermined fraction of its peak value.

The D^+ energy spectrum at 0° has a peak at an ion energy $E \sim 100$ keV and a smoother peak of amplitude smaller by a factor ~ 100 for $1.5 \text{ MeV} \leq E \leq 2 \text{ MeV}$. Less pronounced peaks are observed for $0.1 \text{ MeV} \leq E \leq 1 \text{ MeV}$. The data are obtained from the ion-track distribution on CR-39 or cellulose nitrate targets exposed to a single shot or to multiple shots. At least two different mechanisms of ion acceleration (up to $E \approx 1 \text{ MeV}$) are active during the resistivity surge in the CS. One is experimentally characterized by a nearly constant peak energy/per charge (Z) for different ion species (e.g., H^+ , D^+) and dominates over other acceleration mechanisms in the 0° ion beam. The second is characterized by the same peak velocity v_0 for ions with different values of M/Z and dominates in the 180° ion beam direction of the electron beam. Our experimental data clearly indicate that ions with the lowest value of M/Z are preferentially accelerated at 0° [e.g., with a filling pressure of 50% of H_2 and 50% of D_2 in the discharge chamber the total amount $N_H(0^\circ)$ of H^+ tracks and $N_D(0^\circ)$ of D^+ tracks forming Thomson spectrometer parabola for $0.1 \text{ MeV} \leq E \leq 0.3 \text{ MeV}$ give, typically, $N_H(0^\circ)/N_D(0^\circ) \approx 1.7$]. The situation is completely different at 180° [with the same filling pressure of H_2 and D_2 , the ion track ratio is reversed, i.e., $N_D(180^\circ)/N_H(180^\circ) \approx 1.7$. In this case $N(180)$ is the total amount of tracks observed on one side of the limiting velocity "line" $v=\text{const}=v_0$ of a Thomson-spectrometer target]. The preferential acceleration of D^+ ions over H^+ at 180° is consistent with the observation that ion clusters with a $M/Z \gg 1$ are formed within the beam source and ejected with a typical velocity v_0 . H^+ , D^+ , H , D may evaporate from (and preserve the same velocity v_0 of) ion clusters with $M/Z \gg 1$ which enters the 10^{-5} Torr vacuum chamber of the Thomson spectrometer. The observed fractional composition $N_D(180)/N_H(180)$ of the 180° beam fits the composition of the ion source after the D^+ enrichment of the ion source volume because of the preferential accelerations of H^+ ions at 0° . The reproducibility of the data from hundreds of shots rules out the possibility that this observed coincidence of the H^+/D^+ fractional compositions of 180° beam and source remnants is the casual result of independent events. If we conclude that the 180° beam composition is the source composition at the proper time of emission then this also implies that the ion clusters are ejected after the explosive acceleration process at 0° where ion energies up to 10 MeV are observed, from the same region within the source where the selective process of ion acceleration occurs and within a time interval small enough to prevent a composition change because of ion diffusion from neighbouring regions.

Further evidence of the formation and emission of ion clusters in the dis-integration process of the CS is obtained from: (A) Characterization of etched particle tracks, (B) Pinhole imaging of the ion source from the ion emission and image splitting with a 5 kG magnet inserted between pinhole and image recording plate (CR-39). The magnet (pole dia. 2.5 cm, pinhole dia. 150 μm) splits the pinch image in two equal images - details of sharp boundaries coincide - at a distance of ~ 4 mm from each other. The analyzer field is several orders of magnitude smaller than the self-field B_θ of the pinch. This is consistent with the view that heavy ion clusters (with $M/Z \gg 1$) cross unaffected the pinch field B_θ and then disassemble in a light (D^+) component and other heavy components. Production and propagation of neutrals (from charge exchange) can be ruled out because of the particle energy (from filtering of the ion image). Any alternative to the idea of heavy clusters emission, production and evaporation would imply a distortion of the pinhole image - because of B_θ - which is not observed (our pinhole resolution is 150 μm or better). Time resolved ion spectra are obtained from (A) ion time of flight (Faraday cup method) and (B) from a Thomson spectrometer with a voltage ramp (repetitive pulses with 16 nanosec spacing between pulses) which changes the electric field. Propagation of ion clusters and plasmoids in a 10^{-5} Torr vacuum has been observed both at 0° and 180° by injecting the beam in the vacuum chamber through a 10 millisec opening valve (0.5 mm aperture dia.) or through a 150 μm dia. aperture and differential pumping. Target damage and particle track etching give the changes of the internal structure of the beams which have been analyzed so far up to a propagation distance of ~ 100 cm in the 10^{-5} Torr vacuum.

We have carried out preliminary tests of the PF performance as repetitive opening switch of a > 10 μs current pulse (from a pulse forming network) by increasing of 50% the external inductance between capacitor bank and electrode. With this procedure a train of 4-6 current sheaths (CS) has been obtained. The time spacing between consecutive current sheaths is 0.4-0.8 μs . The 40 kV trigger of the five high-pressure switches for the upgrade (200 kJ) system has been built and the switches are in the construction stage. All the data have been obtained from three PF machines with an identical geometry (Mather type, outer el. dia. 10 cm, inner el. dia. 3.4 cm), two with capacitor banks of 9 kJ at 20 kV and one with a bank of 4 kJ at 20 kV.

Table 1. Neutron yield dependence on knife edge and on knife-edge length L.
Initial voltage 17 kV; filling with 6 Torr of D_2 .

γ	No knife edge, $n_{max} = 5.1 \times 10^8$ $\bar{n} (n > \gamma n_{max})$	Knife edge $L = 7 \text{ mm}, n_{L max}^* = 7.6 \times 10^8$ $\bar{n}_L (n \geq \gamma n_{L max} \pm \sigma)$	Increase $\Delta \bar{n}$ $= \bar{n}_L - \bar{n}$
70%	$4.3 \pm .1 \times 10^8$	$6.3 \pm .4 \times 10^8$	46%
60%	$4.0 \pm .1$	$5.6 \pm .3$	40%
50%	$3.6 \pm .1$	$5.0 \pm .3$	44%
40%	$3.2 \pm .1$	$4.3 \pm .3$	36%
30%	$2.8 \pm .1$	$3.8 \pm .3$	35%
10%	$2.2 \pm .1$	$2.6 \pm .2$	18%

* $n_{L max}$ is the mean value of the neutron yield n_L from the three shots with the highest values of n_L for a specific value of L . $\bar{n}_L (n \geq \gamma n_{L max})$ is the mean value of n_L from all and only the shots with $n_L \geq \gamma n_{max}$.

γ = conveniently chosen percentage.

σ = standard deviation

Tested values of L : 2.5, 7, 12, 17 mm;

Best result with $L = 7 \text{ mm}$

Fig. 1-A Basic Element of Switch

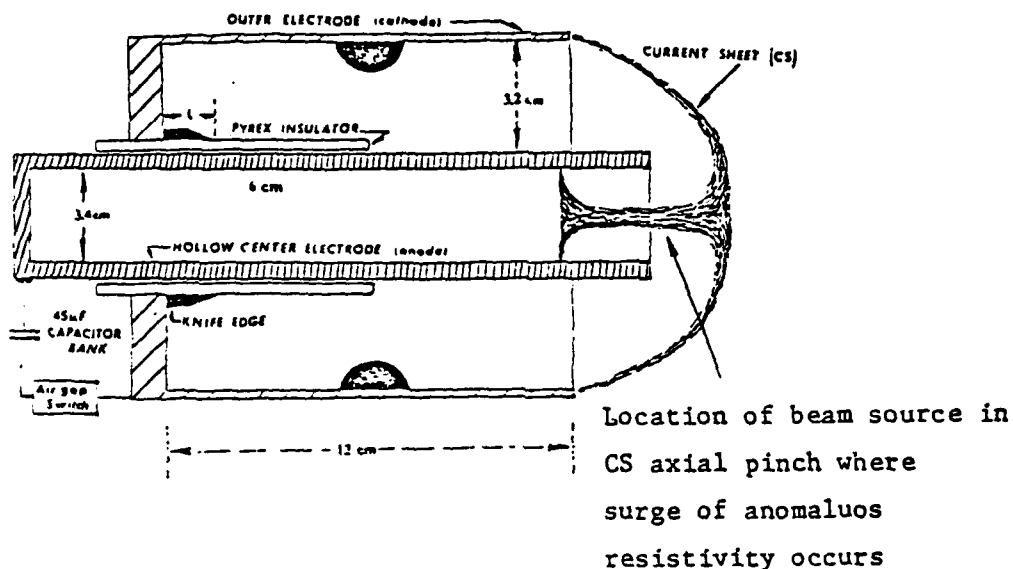
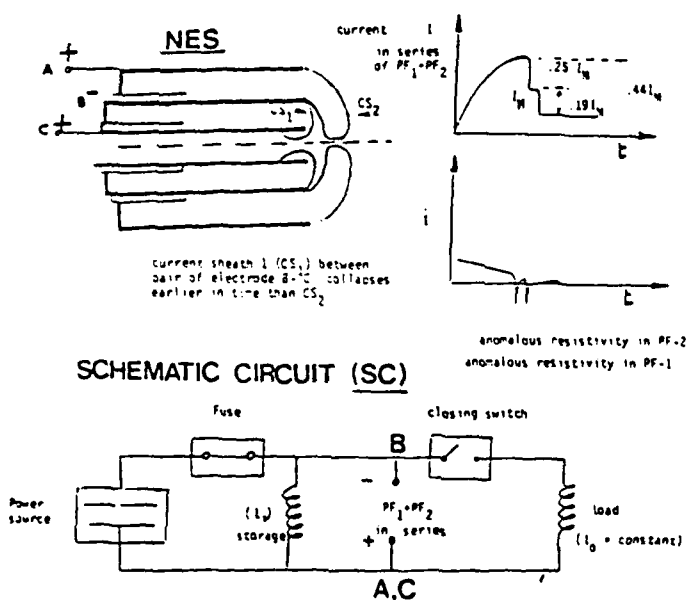


Fig. 1-B: Example of Nested Electrode System (NES) for Series Operation



A,B,C in NES connect to A,B,C in SC

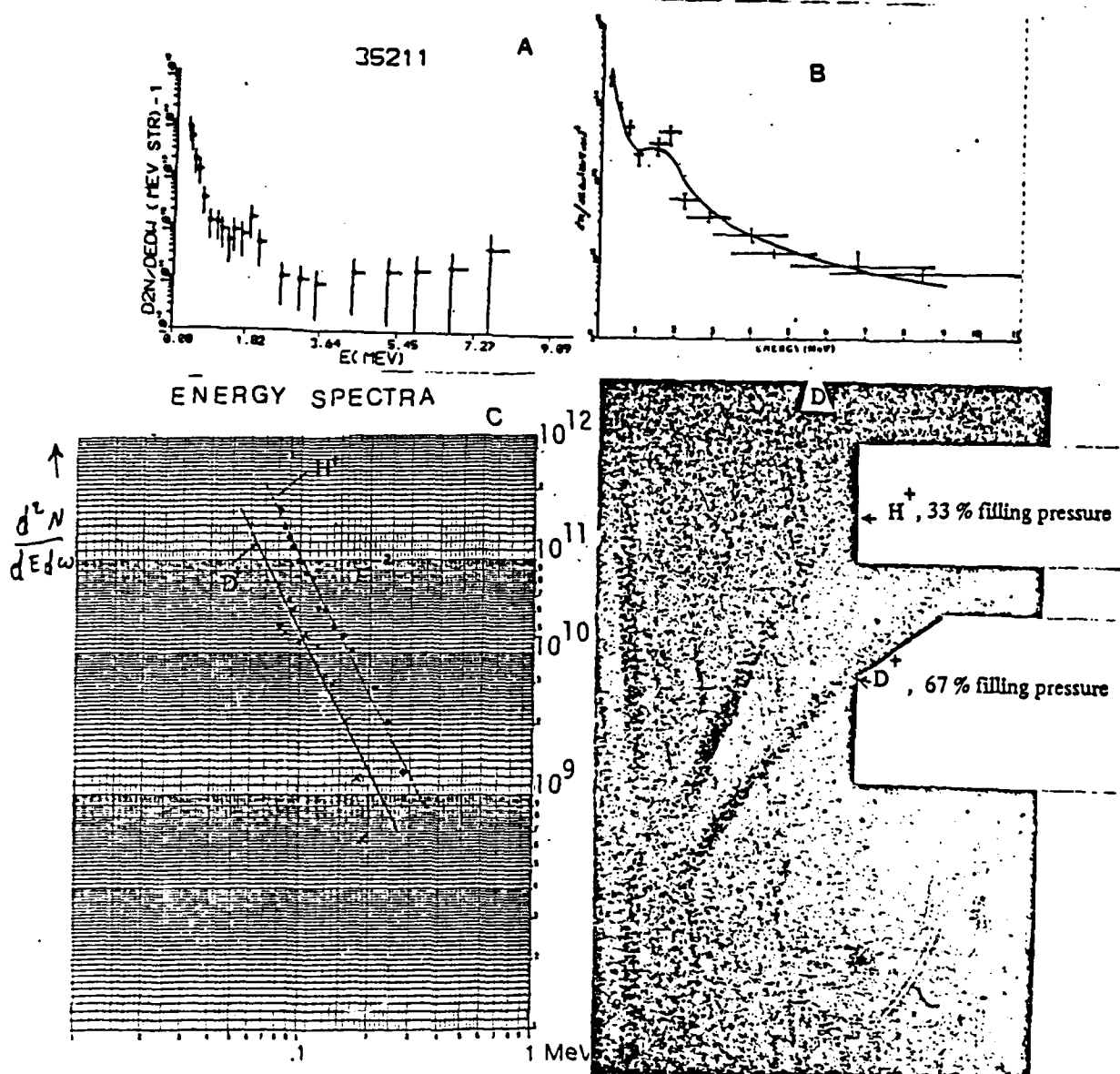


Fig. 2 . A: Ion spectrum from high resolution magnetic analyzer (edge focusing).
 B: Ion spectrum from time of flight method.
 C: Ion spectrum from Thomson spectrometer(0^0), single shot in H_2+D_2 .
 D: Thomson spectrometer parabola distribution (pattern of ion tracks) from which the spectra in C has been derived (filling with 33% of H_2 and 67% of D_2 ; the preferential acceleration of H^+ as compared to D^+ is evident because of the somewhat higher quantity of H^+ tracks in the H^+ parabola (closer to θ_b axis) than that of D^+ in D^+ parabola(see Fig.3)

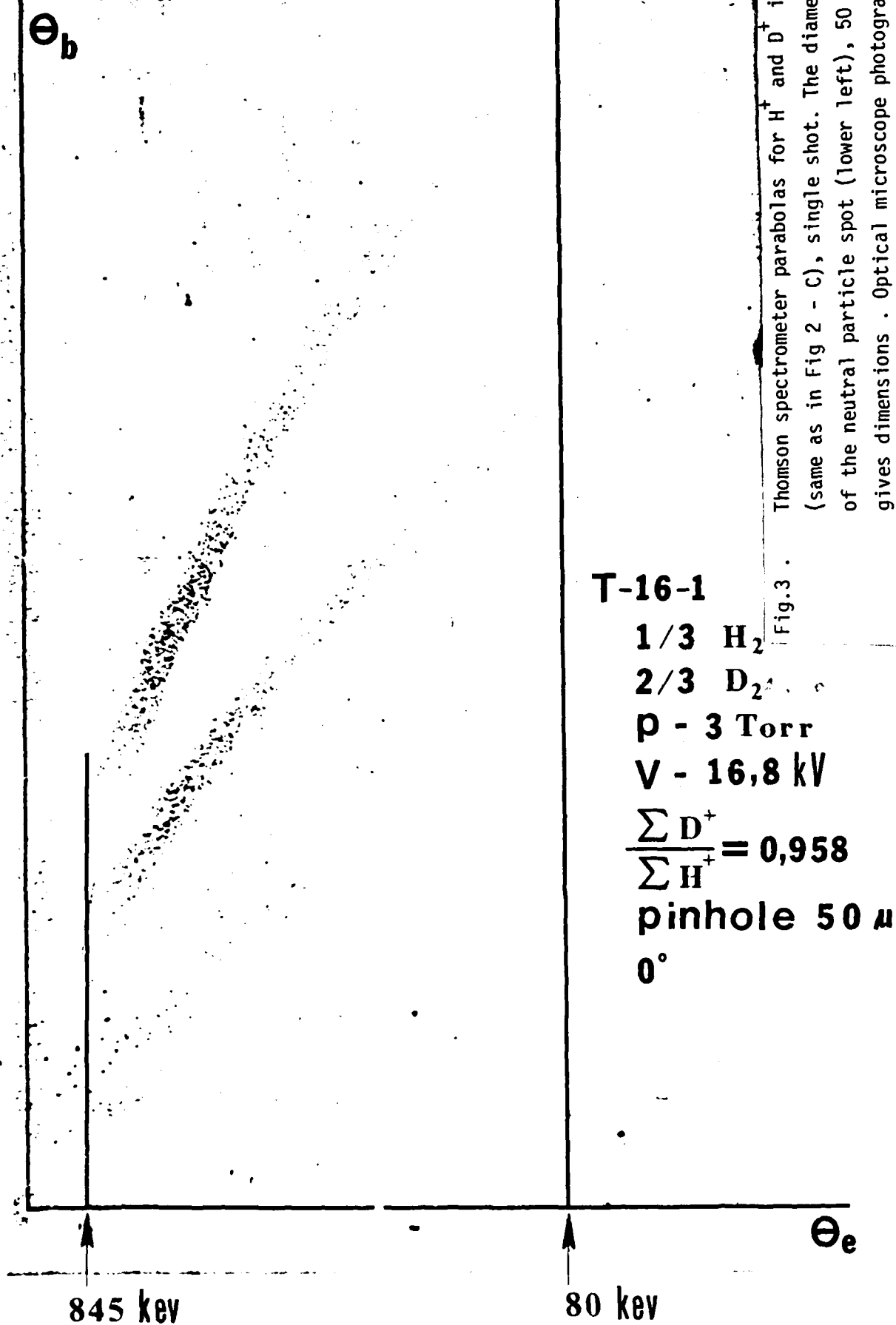


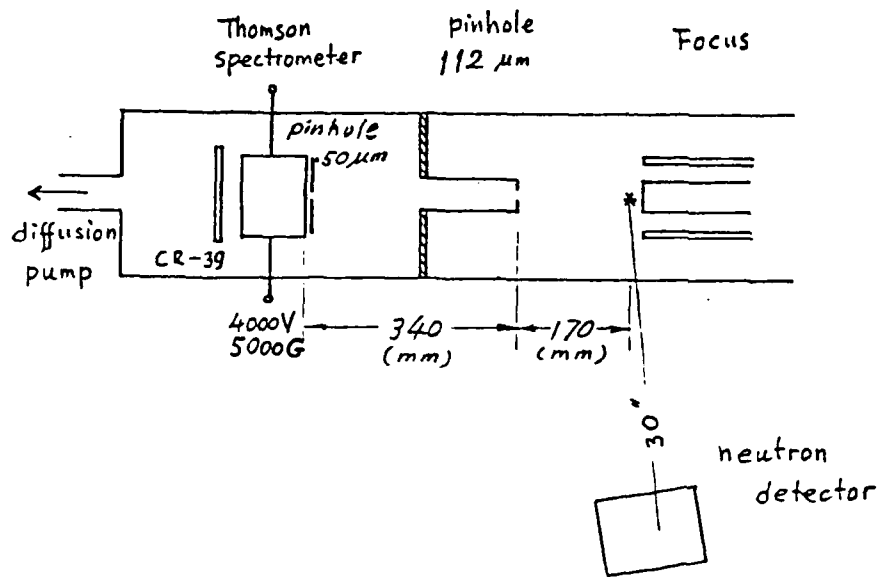
Fig.3 . Thomson spectrometer parabolas for H^+ and D^+ ions
 (same as in Fig 2 - C), single shot. The diameter
 of the neutral particle spot (lower left), 50 μm
 gives dimensions . Optical microscope photograph.
 H^+/D^+ track ratio from track count between vertical
 lines of constant energy per charge E/Z .

Front end of anode



Fig. 3-A. Pinhole image of the ion beam source (45° direction; pinhole dia. 150 μm). A magnetic field orthogonal to the beam direction (8 kG) is inserted immediately behind the pinhole, between pinhole and target(CR-39). This field splits the image in two similar images: An undeflected image along the electrode axis (axis mark at left) and a shifted image (above). The image is formed from the non uniform distribution of etched ion tracks . The ion of the shifted image (D^+) can penetrate a 20 μm thick mylar filter. The unshifted image is wiped out by a 0.1 μm thick formvar filter. The diameter of the ion tracks in the shifted image is 3-5 μm ; the track diameter in the unshifted image is 8-12 μm .

Fig. 4 . Experimental arrangement for tests with Thomson spectrometer at 0° as in Fig. 3, 2-C, 2-D .



The experimental arrangement for tests with the high resolution magnetic analyzer (7-12.5 kG, edge focusing, $dE/E = 0.5\%$, 10 ms opening valve) is described in the literature:

The Plasma Focus as a Source of Collimated Beams of Negative Ion Clusters and of Neutral Deuterium Atoms, V. Nardi, C. Powell, Amer. Inst. of Phys., Proc. Vol 111, (New York, 1984) p. 463.

Ion Imaging and Energy Spectrum from the Plasma Focus Ion Emission, V. Nardi, C. Powell, W. Prior, W. H. Bostick, Controlled Fusion and Plasma Physics, Vol. 70, Part I, p. 489, 1983 (European Physical Soc.).

The experimental arrangement and the method for the derivation of the ion spectrum from time of flight is described in :H. Kilic, Ph.D. Thesis , Stevens Institute of Technology (1984); University Microfilms, P.O.Box1346 Ann Arbor, Michigan 48106, and H.Kilic, V.Nardi, C. Powell , in Press.

Fig. 5 . Thomson spectrometer parabolas from multiple shots (180^0 direction) in a mixture of 50% H_2 and 50% D_2 by filling pressure. The total count of D^+ tracks is greater than the total count of H^+ tracks by a factor ~ 1.7 (the count is made from the high energy point where the parabola originate - on the constant velocity line v_0 - to a point on a constant energy - per-charge line $E/Z = 150$ keV, for both parabolas).

Fig. 5 - A reports the 180^0 spectra (for H^+ and D^+) dN/dE from the parabolas of Fig.5 (relative units; spectrometer acceptance $d\Omega = 2.63 \times 10^{-7}$ sr).

Fig.5 - B reports the experimental set up for target T-98 of Fig.5 (multiple shot exposure). Note that the Thomson spectrometer pinhole is located before the magnet poles in all tests at 180^0 , 90^0 , 70^0 to cope with the relatively small intensity of the ion emission in these directions as compared to the emission intensity at 0^0 (differential pumping is always used).

0.89 cm/ns

constant v_0
line

Θ_b

H^+

D^+

T-98
 $1/2 H_2$
 $1/2 D_2$
 $P - 3 \text{ Torr}$
 $V - 17.5 \text{ kV}$
pinhole 200 μm
 180°

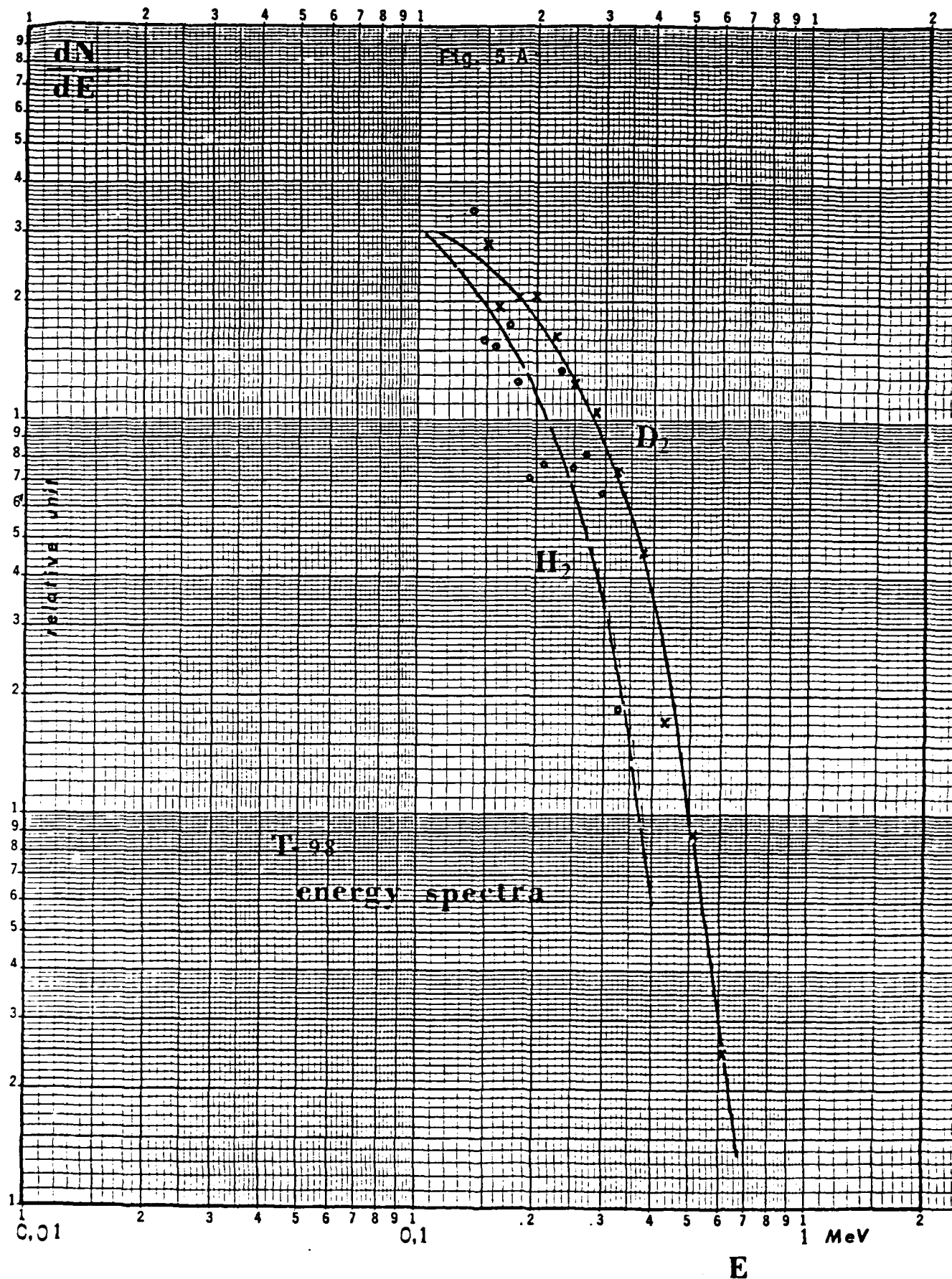


Fig. 5 B

T - 98

180°

pinhole 1
200 μm

pinhole 2
200 μm

THOMSON
SPECTROMETER

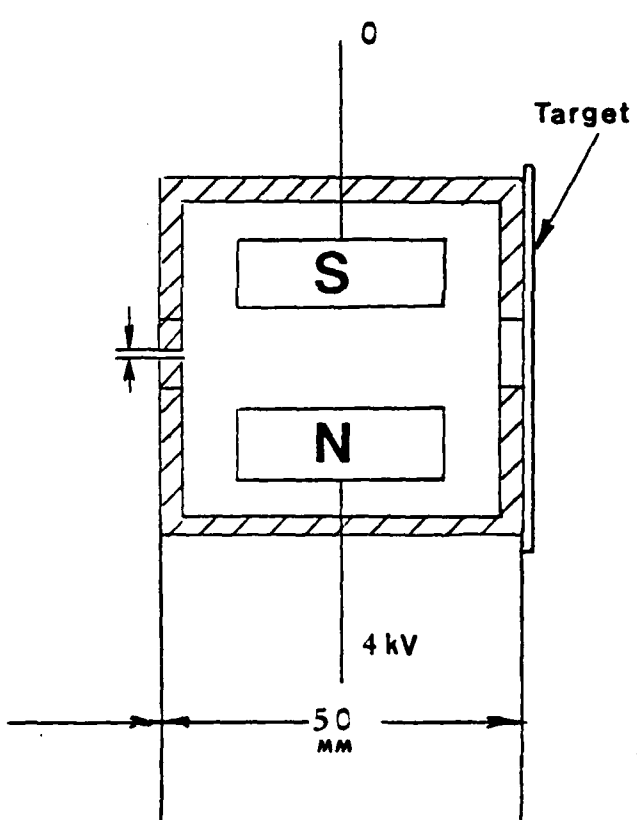
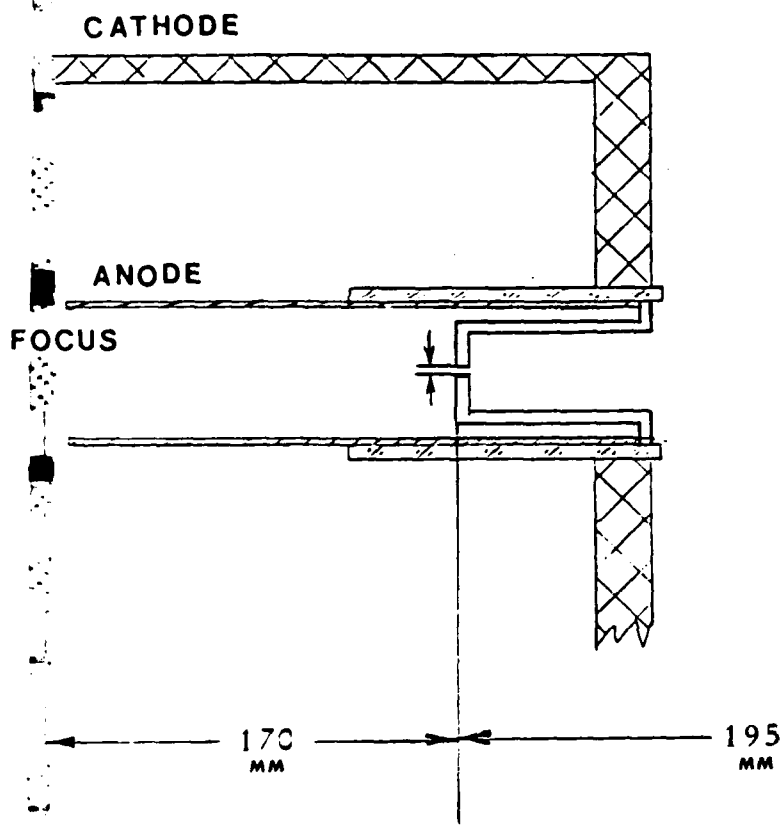


Fig. 6 .

Distorted D^+ parabola from a sequence of voltage pulses (with 17 nanosec between pulses of constant amplitude) applied to the Thomson spectrometer electrodes/poles. The time marks , as indicated, are generated from the voltage peaks.
The difference in the time of emission - time lag $T_L(E_1, E_2)$ - of ions with energy E_1 and the emission time of ions with energy E_2 is deived from the observed time of impact $T(E_1)$, $T(E_2)$ on the target and from the time of flight $t_f(E) = d_0/(2E/M)^{1/2}$ to cover the distance d_0 between source and target;
$$T_L(E_1, E_2) = T(E_1) - t_f(E_1) + - T(E_2) + t_f(E_2) .$$

The D^+ energy spectrum from the distorted parabola of Fig.6 is presented in Fig.6-A and the time lag in Fig. 6-B , (ions with higher energy values are , in this case, emitted later than the ion of lower energy).

Fig.6

Θ_b

Θ_e

$T = -11-2$

$D_2, 3,5 \text{ Torr}$

$V = 16,8 \text{ kV}$

pinhole $50 \mu\text{m}$

0°

90°

180°

270°

360°

450°

540°

630°

720°

810°

900°

990°

1080°

1170°

1260°

1350°

1440°

1530°

1620°

1710°

1800°

1890°

1980°

2070°

2160°

2250°

2340°

2430°

2520°

2610°

2700°

2790°

2880°

2970°

3060°

3150°

3240°

3330°

3420°

3510°

3600°

3690°

3780°

3870°

3960°

4050°

4140°

4230°

4320°

4410°

4500°

4590°

4680°

4770°

4860°

4950°

5040°

5130°

5220°

5310°

5400°

5490°

5580°

5670°

5760°

5850°

5940°

6030°

6120°

6210°

6300°

6390°

6480°

6570°

6660°

6750°

6840°

6930°

7020°

7110°

7200°

7290°

7380°

7470°

7560°

7650°

7740°

7830°

7920°

8010°

8100°

8190°

8280°

8370°

8460°

8550°

8640°

8730°

8820°

8910°

8990°

9080°

9170°

9260°

9350°

9440°

9530°

9620°

9710°

9800°

9890°

9980°

10070°

10160°

10250°

10340°

10430°

10520°

10610°

10700°

10790°

10880°

10970°

11060°

11150°

11240°

11330°

11420°

11510°

11600°

11690°

11780°

11870°

11960°

12050°

12140°

12230°

12320°

12410°

12500°

12590°

12680°

12770°

12860°

12950°

13040°

13130°

13220°

13310°

13400°

13490°

13580°

13670°

13760°

13850°

13940°

14030°

14120°

14210°

14300°

14390°

14480°

14570°

14660°

14750°

14840°

14930°

15020°

15110°

15200°

15290°

15380°

15470°

15560°

15650°

15740°

15830°

15920°

16010°

16100°

16190°

16280°

16370°

16460°

16550°

16640°

16730°

16820°

16910°

17000°

17090°

17180°

17270°

17360°

17450°

17540°

17630°

17720°

17810°

17900°

17990°

18080°

18170°

18260°

18350°

18440°

18530°

18620°

18710°

18800°

18890°

18980°

19070°

19160°

19250°

19340°

19430°

19520°

19610°

19700°

19790°

19880°

19970°

20060°

20150°

20240°

20330°

20420°

20510°

20600°

20690°

20780°

20870°

20960°

21050°

21140°

21230°

21320°

21410°

21500°

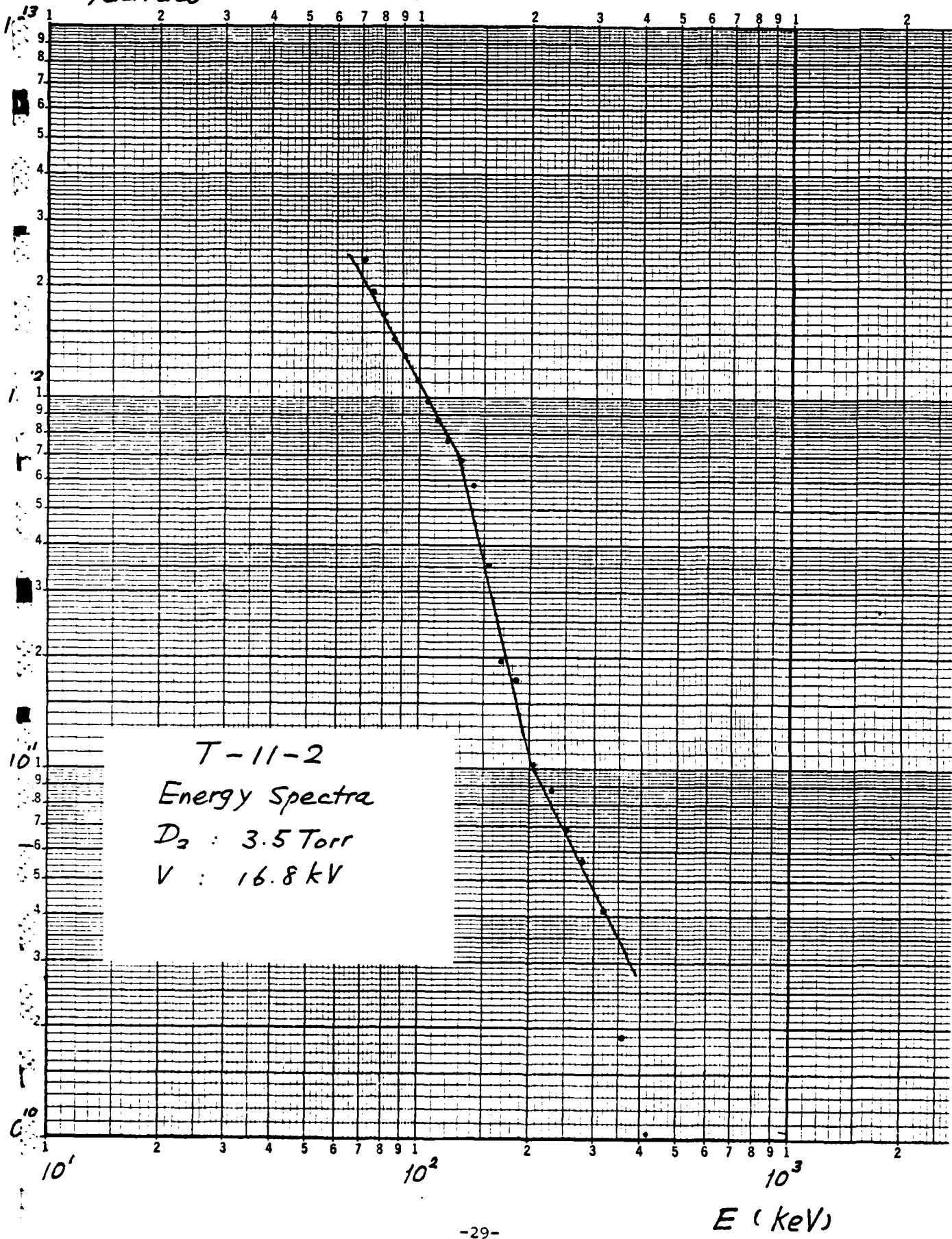
21590°

21680°

21

$d^2N/dE \cdot d\omega$

Fig. 6- A



Target T-11-2

Fig. 6-B

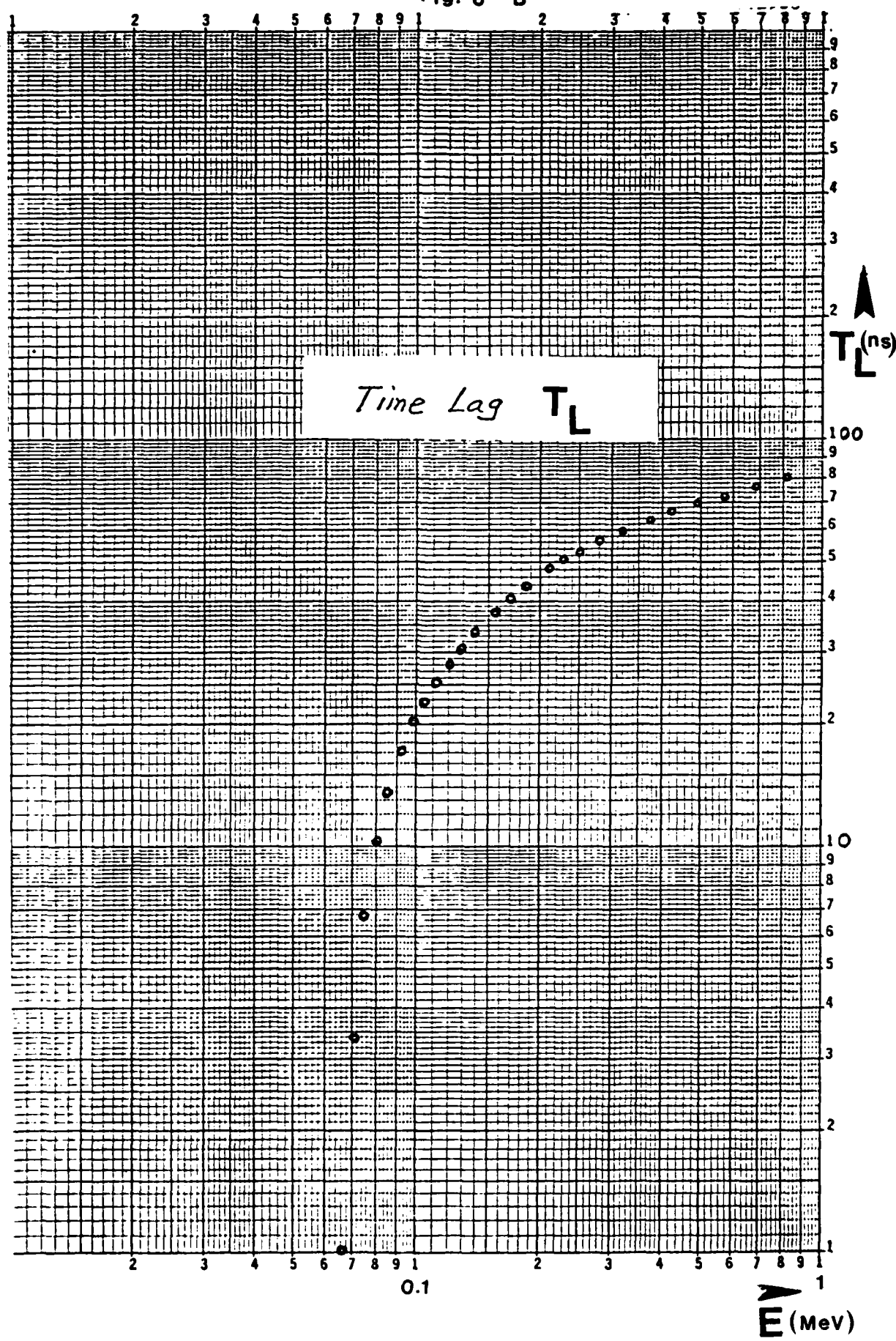


Fig. 7. Thomson spectrometer parabola from a test with electron beam focussing pipe (multiple shots; experimental arrangement as in Fig. 7A).

The ion spectrum has several peaks the largest at 340 keV (the same peak energy of the electron beam).

A low voltage (2 kV instead of 4 kV as for other tests) is applied on Thomson spectrometer electrodes.

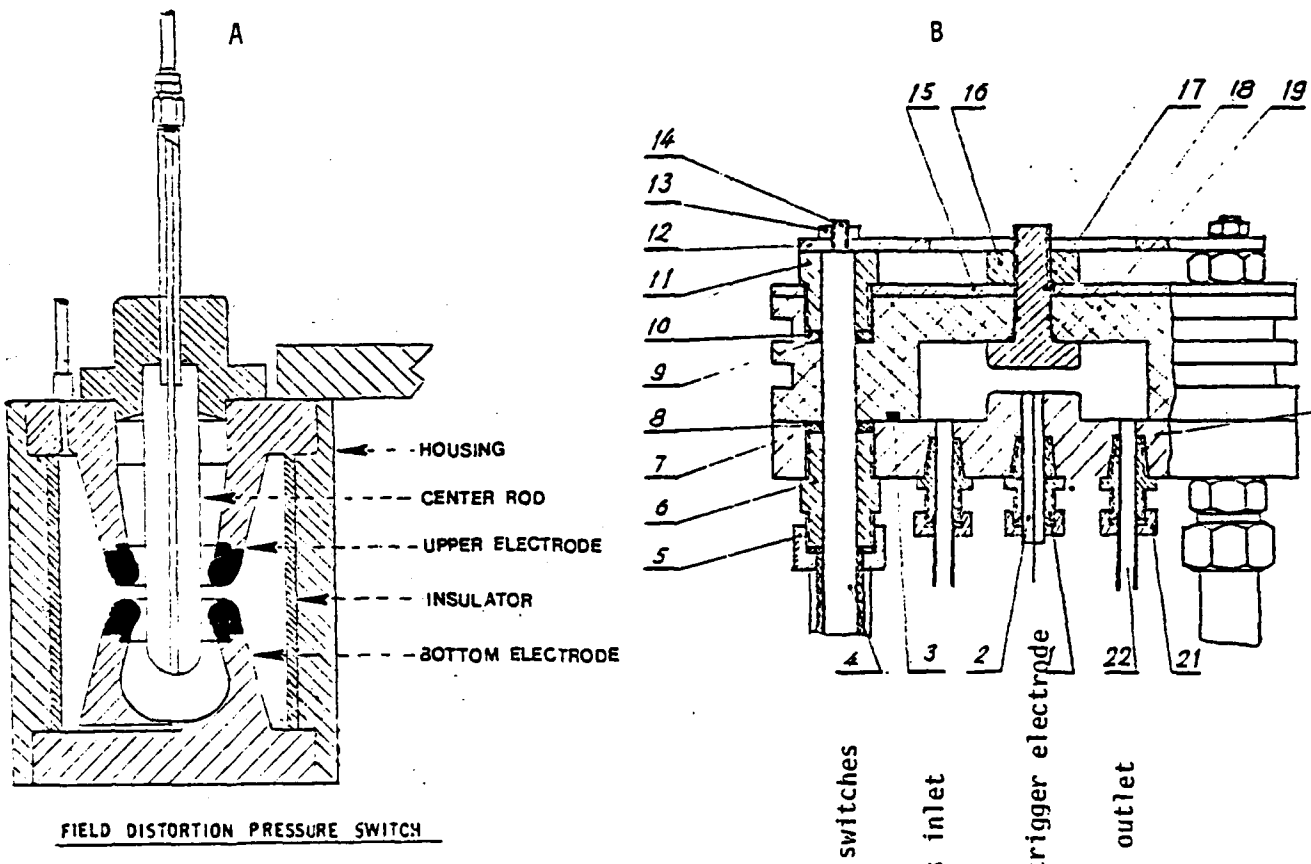
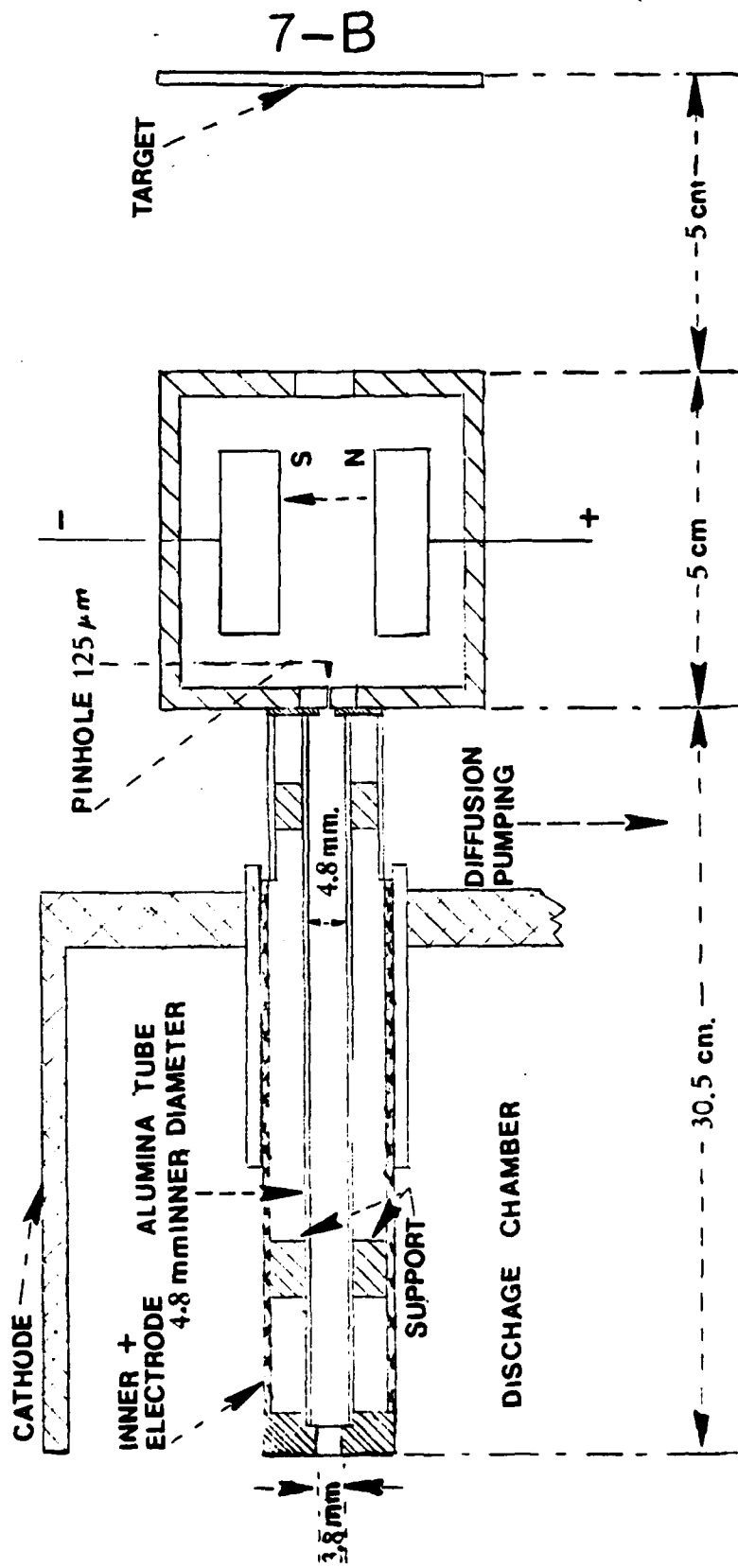


Fig. 8 . One of the five low inductance switches for the upgraded 200 kJ PF system (the dark sections are made of sinter. material), in A. Trigger for the five switches in B .



IN 180° DIRECTION T-74

Publications and Conference Communications 1984

1. V. Nardi: "On Metallic Hydrogen(I)", Int. J. Hydrogen Energy 9, 543 (1984). K. Weil, V. Nardi: "On Metallic Hydrogen (II)", Int. J. Hydrogen Energy 10 (1985).
2. V. Nardi, C. Powell: "The Energy Spectrum of the Plasma Focus Ion Beam at 0°", Invited paper, in press, Fusion Technology, Vol. 6, 1985
3. H. Kilic, V. Nardi, W. Prior: "Energy Analysis of the Ion Beam from the Plasma Focus", 1984 IEEE Internat. Conf. on Plasma Science, Conference Record, IEEE Publication No. 84 CH 1958-8, p. 84 (1984).
4. A. Bortolotti, W. H. Bostick, F. Mezzetti, V. Nardi, W. Prior: "Time Structure of the Particle Beam Source and Current Sheath Filamentation in the Plasma Focus", IEEE Publ. No. 84 CH 1958-8, p. 85 (1985).
5. C. Powell, V. Nardi: "Energy Spectra of D⁺ Ion Beams, High-Z Impurities and Ion Clusters From a Plasma Focus", IEEE Publ. No. 84 CH 1958-8, p. 85 (1984).
6. V. Nardi, J. Feugeas, C. M. Luo, C. Powell: "Propagation of Self-Field-Dominated Beams of Electron and Deuterons", Bull. Am. Phys. Soc. 29, 1233 (1984).
7. A. Bortolotti, W. H. Bostick, A. Fuschini, F. Mezzetti, V. Nardi, C. Powell: "Breakdown-Field Effect on the Neutron Yield and Ion Beams of D₂ Plasma Focus Discharges", Bull. Am. Phys. Soc. 29, 1266 (1984).
8. H. Kilic, V. Nardi, W. Prior: "Characteristic of the Energy Spectrum Between 0.2-9 MeV of the Plasma Focus Ion Beams", Bull. Amer. Phys. Soc. 29, 1266 (1984).

Full Length Papers Accepted for Publication

1. V. Nardi, C. M. Luo, C. Powell: Anisotropy of the Ion Energy Spectrum from Thomson Spectrometers. Proc. 4th Intern. Workshop on Plasma Focus and z-pinch Research, 9-11 Sept. 1985, Warsaw, C. Czekaj and S. Denus, edit.
2. W. H. Bostick, C. M. Luo, V. Nardi, C. Powell (Stevens Tech), A. Bortolotti, A. Fuschini, F. Mezzetti (University of Ferrara), Measurements on Pinhole Camera Photographs with Particle Detectors and Plasma Focus Optimization. Proc. 4th Intern. Workshop (same as above).
3. W. H. Bostick, V. Nardi: The Electromagnetic RAM Action of the Plasma Focus as a Paradigm for the Production of the Cosmic Rays and the Gigantic Jets, Proc. 19th Int. Cosmic Ray Conference, 11-23 Aug. 85, San Diego, CA.

END

FILMED

2-86

DTIC